



**HAL**  
open science

## Masses of the components of SB2 binaries observed with Gaia. III. Accurate SB2 orbits for 10 binaries and masses of HIP 87895

F. Kiefer, J.-L. Halbwachs, Frédéric Arenou, Dimitri Pourbaix, B. Famaey, P. Guillout, Y. Lebreton, A. Nebot Gómez-Morán, Tsevi Mazeh, J.-B. Salomon, et al.

### ► To cite this version:

F. Kiefer, J.-L. Halbwachs, Frédéric Arenou, Dimitri Pourbaix, B. Famaey, et al.. Masses of the components of SB2 binaries observed with Gaia. III. Accurate SB2 orbits for 10 binaries and masses of HIP 87895. *Monthly Notices of the Royal Astronomical Society*, 2016, 458 (3), pp.3272-3281. 10.1093/mnras/stw545 . hal-01291148

**HAL Id: hal-01291148**

**<https://hal.science/hal-01291148>**

Submitted on 3 Mar 2019

**HAL** is a multi-disciplinary open access archive for the deposit and dissemination of scientific research documents, whether they are published or not. The documents may come from teaching and research institutions in France or abroad, or from public or private research centers.

L'archive ouverte pluridisciplinaire **HAL**, est destinée au dépôt et à la diffusion de documents scientifiques de niveau recherche, publiés ou non, émanant des établissements d'enseignement et de recherche français ou étrangers, des laboratoires publics ou privés.

# Masses of the components of SB2 binaries observed with *Gaia*. III. Accurate SB2 orbits for 10 binaries and masses of HIP 87895 \*\*

F. Kiefer<sup>1†</sup>, J.-L. Halbwachs<sup>2</sup>, F. Arenou<sup>3</sup>, D. Pourbaix<sup>5</sup>, B. Famaey<sup>2</sup>, P. Guillout<sup>2</sup>, Y. Lebreton<sup>3,4</sup>, A. Nebot Gómez-Morán<sup>2</sup>, T. Mazeh<sup>1</sup>, J.-B. Salomon<sup>2</sup>, C. Soubiran<sup>6</sup> and L. Tal-Or<sup>1,7</sup>

<sup>1</sup>*School of Physics and Astronomy, Tel Aviv University, Tel Aviv 69978, Israel*

<sup>2</sup>*Observatoire astronomique de Strasbourg, Université de Strasbourg, CNRS, UMR 7550, 11 rue de l'Université, 67000 Strasbourg, France*

<sup>3</sup>*GEPI, Observatoire de Paris, PSL Research University, CNRS, Université Paris Diderot, Sorbonne Paris Cité, Place Jules Janssen, 92195 Meudon, France*

<sup>4</sup>*Institut de Physique de Rennes, Université de Rennes 1, CNRS UMR 6251, F-35042 Rennes, France*

<sup>5</sup>*FNRS, Institut d'Astronomie et d'Astrophysique, Université Libre de Bruxelles, boulevard du Triomphe, 1050 Bruxelles, Belgium*

<sup>6</sup>*Laboratoire d'Astrophysique de Bordeaux, LAB UMR 5804, CNRS, 2 rue de l'Observatoire, BP 89 33270 Floirac, France*

<sup>7</sup>*Institut für Astrophysik (IAG), Friedrich-Hund-Platz 1, D-37077 Göttingen, Germany*

Accepted . Received 2015 ; in original form 2015

## ABSTRACT

In anticipation of the *Gaia* astrometric mission, a large sample of spectroscopic binaries has been observed since 2010 with the SOPHIE spectrograph at the Haute-Provence Observatory. Our aim is to derive the orbital elements of double-lined spectroscopic binaries (SB2s) with an accuracy sufficient to finally obtain the masses of the components with relative errors as small as 1 % when the astrometric measurements of *Gaia* are taken into account. In this paper we present the results from five years of observations of 10 SB2 systems with periods ranging from 37 to 881 days. Using the TODMOR algorithm we computed radial velocities from the spectra, and then derived the orbital elements of these binary systems. The minimum masses of the components are then obtained with an accuracy better than 1.2 % for the ten binaries. Combining the radial velocities with existing interferometric measurements, we derived the masses of the primary and secondary components of HIP 87895 with an accuracy of 0.98% and 1.2% respectively.

**Key words:** binaries: spectroscopic, stars: fundamental parameters stars: individual:HIP 87895

## 1 INTRODUCTION

Mass is the most crucial input in stellar internal structure modelling. It predominantly influences the luminosity of a star at a given stage of its evolution, and also its lifetime. The knowledge of the mass of stars in a non-interacting binary system, together with the assumption that the components have same age and initial chemical composition, allows the age and the initial helium content of the system to be determined and therefore to characterize the structure and evolutionary stage of the components. Such modelling provides insights into the physical processes governing the

structure of the stars. Moreover provided masses are known with great accuracy (Lebreton 2005), it gives constraints on the free physical parameters of the models. Therefore, modelling stars with extremely accurate masses (at the 1 % level), in different ranges of masses, would allow to firmly anchor the models of the more loosely constrained single stars.

This paper is the third in a series dedicated to the derivation of accurate masses of the components of double-lined spectroscopic binaries (SB2) with the forthcoming astrometric measurements from the *Gaia* satellite. In paper I (Halbwachs et al. 2014), we have presented our program to derive accurate masses from *Gaia* and from high-precision spectroscopic observations. We have selected a sample of 68 SB2s for which we expect to derive very precise inclination with *Gaia*, and  $M \sin^3 i$  with the Spectrographe

\* based on observations performed at the Observatoire de Haute-Provence (CNRS), France

† E-mail: flavien@wise.tau.ac.il

pour l’Observation des PHénomènes des Intérieurs Stellaires et des Exoplanètes (SOPHIE spectrograph, Haute-Provence Observatory). Our objective is to determine for these SB2 systems the masses of the two components with an accuracy about 1 %. We have been observing these stars since 2010 with SOPHIE. A first result of our program was the detection of the secondary component in the spectra of 20 binaries which were previously known as single-lined (paper I). A second result was the determination of masses for 2 SB2 with accuracy between 0.26 and 2.4 %, using astrometric measurements from PIONIER and radial velocities from SOPHIE (paper II).

Here, we present the accurate orbits measured for 10 SB2s (Table 1) with periods ranging from 37 to 881 days. After 5 years of observations with SOPHIE, we collected a total of 123 spectra. In addition, a large number of previously published measurements is available for each of them in the SB9 catalog (Pourbaix et al. 2004). Four of these targets are new SB2 identified in paper I, and previously known as SB1. Finally, we combined the radial velocity (RV) measurements of one star (HIP 87895) with existing interferometric measurements and derive the masses of the two components.

The observations are presented in Section 2. The method of measurements of radial velocities from SOPHIE’s observations is explained in Section 3. We derive the orbital solutions in Section 4, discussing in particular the issue of the uncertainties when combining different datasets from different instruments. The derivation of the masses of HIP 87895 is discussed in Section 5. Finally, we summarize and conclude on our findings in Section 6.

## 2 OBSERVATIONS

The observations were performed at the T193 telescope of the Haute-Provence Observatory, with the SOPHIE spectrograph. SOPHIE is dedicated to the search of extrasolar planets, and, thanks to its high resolution ( $R \sim 75,000$ ), it enables accurate stellar radial velocities to be measured for SB2 components.

The spectra were all reduced through SOPHIE’s pipeline, including localization of the orders on the frame, optimal order extraction, cosmic-ray rejection, wavelength calibration, flat-fielding and bias subtraction. The minimum signal-to-noise ratio (SNR) is 40 for the faintest stars of the sample, but it may be as large as 150 for a 6-magnitude star. Before each observation run ephemerides were derived from existing orbits provided by the SB9 catalogue (Pourbaix et al. 2004), and priority classes were assigned on the basis of the orbital phase. Four classes were used: the lowest priority corresponds to stars with expected RVs of primary and secondary component sufficiently different to permit accurate measurements, and the highest priority is reserved to the observations of the periastron of eccentric orbits.

Among all the observed SB2, we have selected those which were observed over at least one period, and which received a minimum of 11 observations. Table 1 summarizes this information. Given the very high quality of the measurements, an SB2 orbit could be derived in principle from only 6 of those observations, provided they were made at the most relevant phases. However, we show in Section 4 that 11

**Table 1.** The ten SB2 analyzed in this paper.

HIP	HD	V (mag.)	Period <sup>a</sup> (day)	$N_{\text{spec}}$ <sup>b</sup>	Time span <sup>c</sup> (period)	SNR <sup>d</sup>
<i>Previously published SB2</i>						
12081	15850	7.72	443.49	11	3.3	80
17732	23626	6.27	277.89	11	5.5	120
56275	100215	7.99	47.88	13	30.7	80
87895	163840	6.33	880.78	14	2.1	120
95575	183255	8.05	166.36	13	11.9	75
100321	195850	7.02	37.94	11	45.3	80
<i>SB2 identified in paper I, previously published as SB1</i>						
13791	18328	8.87	48.71	13	28.8	40
61727	110025	7.58	54.88	12	28.3	80
62935	120005	8.53	139.00	11	10.6	40
67195	120005	6.50	39.28	14	37.3	120

<sup>a</sup> The period values are taken from the SB9 catalog (Pourbaix et al. 2004).

<sup>b</sup>  $N_{\text{spec}}$  gives the number of spectra collected with SOPHIE.

<sup>c</sup> The time span is the total span of observation epochs, counted in number of periods.

<sup>d</sup> SNR is the median signal-to-noise ratio of each sample.

observations are necessary to validate the RV uncertainties, and to correct them when necessary.

## 3 RADIAL VELOCITY MEASUREMENTS

The radial velocities of the components are derived using the Two-Dimensional CORrelation algorithm TODCOR (Zucker & Mazeh 1994; Zucker et al. 2004). It calculates the cross-correlation of an SB2 spectrum and two best-matching stellar atmosphere models, one for each component of the observed binary system. This two-dimensional cross-correlation function (2D-CCF) is maximized at the radial velocities of both components. The multi-order version of TODCOR, named TODMOR (Zucker et al. 2004), determines the radial velocities of both components from the gathering of 2D-CCF obtained from each order of the spectrum.

All SOPHIE multi-orders spectra were corrected for the blaze using the response function provided by SOPHIE’s pipeline; then for each of them, the pseudo-continuum was detrended using a p-percentile filter (paper II, or e.g. Hodgson et al. (1985)).

For both components of each binary, we determined a best-matching theoretical spectra from the PHOENIX stellar atmosphere models (Husser et al. 2013). We optimized the 2D-CCF with respect to effective temperature  $T_{\text{eff}}$ , rotational broadening  $v \sin i$ , metallicity  $[\text{Fe}/\text{H}]$ , surface gravity  $\log(g)$ , and flux ratio at 4916 Å,  $\alpha = F_2/F_1$ . Furthermore, each theoretical spectrum is convolved with the instrument line spread function, here modeled by a Gaussian, and pseudo-continuum detrended like the observed spectrum. The spectral parameters obtained through this method are given in Table 2. We determined spectral parameters from 4 spectra per binary on average, with the two components well individualized. The values and their uncertainties given in Table 2 are the average and standard deviation of the individual estimations. The  $1\sigma$  uncertainties do not include known systematics of theoretical models with respect to real spectral types (see e.g. Torres et al. (2012)).

**Table 2.** The stellar parameters determined by optimization of the 2D-CCF obtained with TODMOR. Explanations in Section 3.

HIP	$T_{\text{eff},1}$	$\log g_1$	$V_1 \sin i_1$ <sup>a</sup>	[Fe/H]	$\alpha$
HD	$T_{\text{eff},2}$	$\log g_2$	$V_2 \sin i_2$ <sup>a</sup>	(dex)	(flux ratio)
	(K)	(dex)	(km s <sup>-1</sup> )		
12081	6290	4.24	11.9	-0.37	0.635
15850	± 23	±0.05	±0.1	±0.01	±0.012
	6003	4.30	6.5		
	± 13	±0.01	±0.1		
13791	6173	4.31	5.5	-0.34	0.034
18328	± 6	±0.01	±0.1	±0.01	±0.001
	4953	5.09	0		
	± 95	±0.01			
17732	6030	3.34	9.4	-0.71	0.258
23626	± 7	±0.03	±0.1	±0.01	±0.004
	6051	3.84	0		
	± 18	±0.01			
56275	6889	3.93	20.6	-0.33	0.036
100215	± 36	±0.11	±1	±0.01	±0.002
	4906	4.33	0		
	± 75	±0.01			
61727	6461	3.82	9.8	-0.48	0.070
110025	± 31	±0.15	±0.1	±0.06	±0.007
	5256	4.31	7.7		
	± 168	±0.14	1.4		
62935	5818	4.03	4.9	-0.27	0.054
112138	± 85	±0.08	±0.4	±0.01	±0.015
	4378	4.40	0		
	± 115	±0.13			
67195	6411	4.29	13.6	-0.21	0.027
120005	± 29	±0.13	±0.2	±0.03	±0.002
	4478	4.72	4.5		
	± 418	±0.21	±0.1		
87895	5970	4.33	4.7	-0.19	0.036
163840	± 1	±0.01	±0.1	±0.01	±0.004
	4385	4.81	0		
	± 134	±0.04			
95575	4908	4.75	3.4	-0.88	0.431
183255	± 5	±0.03	±0.1	±0.01	±0.008
	4088	4.51	0		
	± 5	±0.03			
100321	6485	4.17	14.2	-0.39	0.207
195850	± 6	±0.05	±0.2	±0.01	±0.011
	5558	4.39	5.5		
	± 62	±0.04	± 1		

<sup>a</sup> A null value is given to  $V \sin i$  with no error bar whenever found less than SOPHIE's typical pixel size  $\sim 2 \text{ km s}^{-1}$ .

It is worth mentioning that the derived metallicity [Fe/H] is systematically subsolar. Optimizing the CCF of several spectra of the Sun obtained by observing Vesta and Ceres with SOPHIE gave spectral parameters consistent with the known values for the Sun except metallicity that was found to be -0.33 dex. However, we kept the values of metallicity that maximized the 2D-CCF, as given in Table 2.

We then applied TODMOR to all multi-order spectra of each target and determined the radial velocities of both components discarding all orders harboring strong telluric lines. For each of the non-discarded orders, we calculated a two dimensional cross-correlation function, and used the maximum of this function to derive radial velocities for the pri-

mary and the secondary. Final velocities for each component are obtained by averaging these measurements and incorporating a correction for order-to-order systematics – typically 200–500 m s<sup>-1</sup>. The final velocities are displayed in Table 3. They are used to derive the orbital solutions for the 10 SB2 in the next section.

## 4 DERIVATION OF THE ORBITS

The orbital solutions for the 10 SB2 are derived by combining the new measurements presented in this paper with previously published RVs (references in Table 4).

Since several datasets coming from different instruments are used together to derive a common orbital solution, realistic errors should be attributed to each dataset properly. It is explained in the following section. This process guarantees that each dataset receives the proper weight with respect to all others, including the new SOPHIE measurements presented here.

### 4.1 Correction of uncertainties

Uncertainties of previously published measurements, when provided, are usually underestimated. On the other hand, many lists of RV measurements do not include uncertainties, but only weights (W). Therefore, two different procedures are applied to attribute correct uncertainties to these retrieved measurements. They are both based on the calculation of the  $F_2$  estimator of the goodness-of-fit (see Paper II, equation 1, or Stuart & Ord 1994):

- When the uncertainties are provided, a noise is quadratically added to the original uncertainties, in order to get exactly  $F_2=0$  for the SB1 orbit of each component. Since the original uncertainties are underestimated, this results in decreasing the variations of the relative weights of the measurements of a given component.
- When only weights are given, they are first converted to uncertainties ( $\sigma = \sqrt{1/W}$ ). Then they are scaled in order to get  $F_2=0$  for the SB1 orbit of each component.

After this transformation, the SB2 orbit is derived, and  $F_2$  is considered again. The final uncertainties are obtained by multiplying the ones derived above with a factor chosen in order to get  $F_2=0$ . All these operations result in applying the following formulae:

$$\sigma_{RV,1}^{\text{corr}} = \varphi_1 \times \sqrt{\sigma_{RV,1}^2 + \varepsilon_1^2} \quad (1)$$

$$\sigma_{RV,2}^{\text{corr}} = \varphi_2 \times \sqrt{\sigma_{RV,2}^2 + \varepsilon_2^2} \quad (2)$$

Table 4 lists the derived values of the correction terms  $\varphi_1$ ,  $\varphi_2$ ,  $\varepsilon_1$  and  $\varepsilon_2$  for all stars of our sample.

The same procedure is applied to the uncertainties derived by TODMOR for the new measurements. For two binaries (HIP 67195 and HIP 100321), the SB1 orbit of the secondary component leads to a negative value of  $F_2$ , implying that the uncertainties are slightly overestimated. In order to get  $F_2=0$ , we preferred to keep the relative weights fixed, and simply multiply the uncertainties by a coefficient  $\varphi_2$  lower than 1.

**Table 3.** New radial velocities from SOPHIE and obtained with TODMOR. Outliers are marked with an asterisk (\*) and are not taken into account in the analysis.

HIP 12081							HIP 13791						
BJD	$RV_1$	$\sigma_{RV1}$	$RV_2$	$\sigma_{RV2}$	$O_1 - C_1$	$O_2 - C_2$	BJD	$RV_1$	$\sigma_{RV1}$	$RV_2$	$\sigma_{RV2}$	$O_1 - C_1$	$O_2 - C_2$
-2400000	km s <sup>-1</sup>	-2400000	km s <sup>-1</sup>										
55440.6175	-19.3006	0.0348	4.5327	0.0179	0.0498	0.0052	55605.3577	-21.0198	0.0155	12.5004	0.2343	-0.0602	-0.3409
55532.3450	5.2930	0.0401	-22.3033	0.0200	-0.0023	-0.0206	55784.6009	-8.0152*	0.0119*	0.2619*	0.2294*	-0.1650*	9.5587*
55605.3276	-3.1655	0.0775	-13.1499	0.0355	-0.0492	-0.0175	55864.4964	-0.6383	0.0104	-21.6297	0.1661	0.0092	-0.1697
55784.5923	-16.8235	0.0334	2.0058	0.0190	0.2120	-0.0034	55965.3042	4.6405	0.0114	-30.1618	0.1654	0.0038	0.2217
55864.4742	-22.3574	0.0424	7.7735	0.0166	-0.0294	0.0069	56148.6243	-13.0655	0.0099	-0.6196	0.1373	0.0105	-0.1477
55933.2302	11.2363	0.0450	-28.6746	0.0186	0.0576	0.0081	56243.4109	-16.3507	0.0099	5.5330	0.1533	0.0154	0.4489
55966.2854	6.7183	0.0361	-23.8320	0.0214	0.0144	-0.0170	56323.3367	-15.3310	0.0114	3.6038	0.1777	-0.0089	0.2826
56148.6082	-11.1919	0.1043	-4.4740	0.0530	-0.0939	-0.0243	56525.5659	-22.8333	0.0117	15.9524	0.1816	0.0041	-0.0597
56243.3824	-18.1414	0.0393	3.3409	0.0191	0.1222	-0.0043	56526.6076	-22.7883	0.0113	15.7956	0.1800	0.0231	-0.1728
56323.3304	-20.6003	0.0384	5.8376	0.0160	-0.0433	-0.0025	56618.4809	-20.1445	0.0113	11.3540	0.1775	-0.0036	-0.1047
56889.6346	1.3632	0.0490	-18.2750	0.0237	-0.2906	0.0463	56701.3400	9.2144	0.0116	-36.7152*	0.2370*	0.0088	1.3839*
							56890.6072	4.3730	0.0110	-30.1670	0.1576	-0.0229	-0.1901
							57009.3890	-21.3907	0.0112	13.7637	0.1722	0.0158	0.1678

HIP 17732							HIP 56275						
BJD	$RV_1$	$\sigma_{RV1}$	$RV_2$	$\sigma_{RV2}$	$O_1 - C_1$	$O_2 - C_2$	BJD	$RV_1$	$\sigma_{RV1}$	$RV_2$	$\sigma_{RV2}$	$O_1 - C_1$	$O_2 - C_2$
-2400000	km s <sup>-1</sup>	-2400000	km s <sup>-1</sup>										
55532.4636	-22.8766	0.0095	21.9980	0.0170	0.0019	-0.0197	55692.3811	7.9257	0.0226	-64.5112	0.1000	0.3626	0.0800
55784.6076	-22.5330	0.0105	21.6484	0.0215	0.0016	0.0584	55863.6796	-46.4777	0.0309	35.6378	0.1108	0.2361	-0.0068
55933.2851	12.7972	0.0135	-22.2329	0.0328	0.0123	0.0946	55933.6492	6.6220	0.0266	-63.0758	0.0791	0.0026	-0.2274
55965.3166	12.1605	0.0099	-21.5826	0.0163	0.0003	-0.0318	55966.5170	-36.2910	0.0297	17.1534	0.1229	0.5121	-0.1887
56243.4535	12.1444	0.0089	-21.5210	0.0189	0.0060	0.0026	56243.6608	-41.0739	0.0280	24.3508	0.1038	-0.4721	-0.0067
56323.3438	-16.6398	0.0178	14.2097	0.0550	0.0020	-0.0529	56323.5683	-2.5587	0.0224	-44.7952	0.1061	0.4674	0.2403
56525.5908	11.5734	0.0103	-20.8293	0.0201	-0.0154	0.0110	56413.3606	6.2006	0.0221	-61.4924	0.0961	0.2601	0.1022
56618.4465	-22.5381	0.0096	21.6251	0.0163	-0.0060	0.0382	56414.3535	4.4350	0.0239	-59.8103	0.0548	-0.4309	-0.2002
56890.6164	-20.9656	0.0110	19.5609	0.0322	0.0023	-0.0809	56700.5640	5.7582	0.0178	-61.8093	0.1047	-0.3363	0.0697
57009.3996	7.0245	0.0163	-15.2479	0.0403	-0.0123	-0.0676	57009.6387	-39.1607	0.0248	22.8202	0.0789	0.6746	-0.1217
57073.3157	12.5569	0.0093	-22.0421	0.0166	0.0009	0.0008	57073.4672	-7.8378	0.0291	-37.3543	0.1066	-0.6925	0.0742
							57159.4023	-49.4717	0.0484	39.0880	0.1873	-1.1735	0.5173
							57160.3715	-46.9715	0.0302	37.0594	0.0909	0.5892	-0.1492

HIP 61727							HIP 62935						
BJD	$RV_1$	$\sigma_{RV1}$	$RV_2$	$\sigma_{RV2}$	$O_1 - C_1$	$O_2 - C_2$	BJD	$RV_1$	$\sigma_{RV1}$	$RV_2$	$\sigma_{RV2}$	$O_1 - C_1$	$O_2 - C_2$
-2400000	km s <sup>-1</sup>	-2400000	km s <sup>-1</sup>										
55605.5848	-12.6740	0.0136	15.9258	0.1301	-0.0215	-0.3118	55605.6068	-12.3906	0.0106	19.1954	0.1083	-0.0079	0.5511
55693.3588	6.5327	0.0074	-13.5889	0.0846	-0.0088	0.3627	55933.7034	12.2587	0.0212	-16.6646	0.2002	-0.0453	1.0353
55933.6598	-18.4952	0.0158	25.9363	0.2306	-0.0041	0.5154	55965.6957	10.9649	0.0108	-15.5176	0.1105	-0.0205	0.2413
55965.6569	10.2366	0.0092	-19.6786	0.1063	0.0244	0.0466	56034.4799	-9.0670	0.0119	14.7234	0.1188	0.0067	0.9506
56034.4583	-36.6083	0.0087	53.6952	0.1865	-0.0076	-0.2096	56323.6219	-4.1875	0.0106	6.9054	0.1110	-0.0224	0.3592
56323.6069	3.8442	0.0121	-10.5547	0.1624	0.0030	-0.8501	56413.4178	-10.6338	0.0108	16.6760	0.1052	0.0037	0.6010
56413.4059	-12.8533	0.0134	16.2369	0.1274	-0.0334	-0.2641	56414.3653	-10.9714	0.0109	17.2867	0.1098	-0.0001	0.7203
56700.6043	-25.6469	0.0089	36.5198	0.1158	0.0088	-0.1701	56619.6800	6.6032	0.0110	-8.7968	0.1128	0.0060	0.5014
56764.3934	7.9839	0.0082	-15.9285	0.1737	0.0235	0.2550	56700.6311	-12.9241	0.0105	19.9558	0.1044	0.0065	0.5048
57009.6713	8.0070	0.0086	-15.9493	0.1395	0.0020	0.3044	56763.4730	9.7161	0.0103	-13.3344	0.1035	0.0370	0.5012
57073.5033	-19.5056	0.0071	27.7723	0.2897	0.0283	0.7111	57073.5373	14.0341	0.0094	-19.3651	0.0930	0.0212	0.8509
57159.4393	18.4660	0.0089	-32.9927	0.2474	-0.0225	-0.2502							

HIP 67195							HIP 87895						
BJD	$RV_1$	$\sigma_{RV1}$	$RV_2$	$\sigma_{RV2}$	$O_1 - C_1$	$O_2 - C_2$	BJD	$RV_1$	$\sigma_{RV1}$	$RV_2$	$\sigma_{RV2}$	$O_1 - C_1$	$O_2 - C_2$
-2400000	km s <sup>-1</sup>	-2400000	km s <sup>-1</sup>										
55693.4447	-25.3810	0.0201	17.8880	0.1602	-0.0487	0.0120	55306.5401	-25.5851	0.0102	-42.7398	0.1192	-0.0824	-0.2769
55965.7213	-24.1047	0.0187	15.6821	0.1456	-0.0092	-0.0474	55440.3398	-24.3803	0.0107	-44.3309	0.1369	0.0012	-0.1582
56033.4718	-16.6905	0.0198	2.8186	0.1299	-0.0100	-0.0424	55692.5686	-47.1465	0.0103	-9.8598	0.1237	-0.0269	-0.3621
56323.6540	-25.6179	0.0185	18.4821	0.1453	0.0131	0.0876	55783.4403	-41.7373	0.0102	-17.4182	0.1176	-0.0231	0.3225
56323.7172	-25.6252	0.0185	18.4805	0.1502	0.0034	0.0902	56034.6403	-29.2514	0.0104	-37.8613*	0.1264*	-0.0441	-1.0478*
56324.4871	-25.4322	0.0209	18.0313	0.1648	0.0304	-0.0709	56148.4136	-26.2422	0.0103	-41.3782	0.1288	0.0258	-0.0824
56324.5606	-25.4128	0.0196	18.0605	0.1480	0.0177	0.0141	56243.2450	-24.6700	0.0105	-43.8842	0.1276	0.0358	-0.2061
56413.4778	3.2056	0.0197	-31.8507	0.1488	0.0263	-0.2456	56324.6564	-24.3659	0.0121	-44.1758	0.1547	0.0306	-0.0261
56414.4222	0.2645	0.0192	-26.3836	0.1566	0.0138	0.1391	56413.6297	-26.9424	0.0104	-40.1199	0.1358	0.0005	0.1468
56526.3286	55.7540	0.0209	-122.9667	0.1516	-0.0025	-0.1150	56414.5000	-26.9901	0.0104	-39.9479	0.1370	0.0080	0.2346
56763.4478	26.5703	0.0184	-71.9675	0.1492	0.0100	0.2148	56414.5337	-26.9911	0.0104	-40.0227	0.1364	0.0091	0.1564
57073.5916	-18.4045	0.0182	5.7351	0.1389	-0.0178	-0.0869	56525.3681	-42.7839	0.0103	-16.1425	0.1206	-0.0066	-0.0228
57159.4122	4.9344	0.0192	-34.5608	0.1357	0.0026	0.0858	56763.6370	-35.3359	0.0103	-27.2716	0.1088	0.0394	0.1357
57160.4048	1.4943	0.0193	-28.7538	0.1452	-0.0216	-0.0354	57159.5261	-24.3802	0.0103	-43.9809	0.1341	0.0306	0.1471

**Table 3.** Continued.

HIP 95575							HIP 100321						
BJD	$RV_1$	$\sigma_{RV1}$	$RV_2$	$\sigma_{RV2}$	$O_1 - C_1$	$O_2 - C_2$	BJD	$RV_1$	$\sigma_{RV1}$	$RV_2$	$\sigma_{RV2}$	$O_1 - C_1$	$O_2 - C_2$
-2400000	km s <sup>-1</sup>	-2400000	km s <sup>-1</sup>										
55306.6052	-78.1722*	0.0068*	-50.6807*	0.0274*	-0.9557*	-0.9533*	55440.4025	17.4467	0.0262	-20.6978	0.0354	-0.0453	-0.0053
55440.3855	-69.9864	0.0107	-57.8756	0.0514	-0.0113	-0.0413	55693.6211	-30.5121	0.0269	42.2770	0.0338	-0.1057	0.0121
55693.5658	-60.6375	0.0103	-68.3909	0.0740	-0.0148	-0.0863	56147.4444	-33.9387	0.0172	46.9496	0.0192	0.0303	0.0021
55784.4181	-74.6558	0.0069	-52.5504	0.0199	0.0121	0.0302	56243.2764	32.2481	0.0242	-40.0539	0.0329	0.0321	-0.0083
56034.5983	-57.5141	0.0103	-71.8023	0.0453	0.0156	-0.0350	56414.6090	-30.0393	0.0214	41.7375	0.0272	-0.0196	-0.0191
56147.4329	-76.3749	0.0070	-50.6872	0.0298	0.0013	-0.0191	56525.4060	-35.5108	0.0223	49.0625	0.0234	0.0698	-0.0032
56243.2640	-51.3445	0.0075	-78.6904	0.0286	-0.0033	0.0051	56526.4184	-34.6986	0.0204	47.8903	0.0271	-0.0222	0.0130
56414.5737	-53.1692	0.0091	-76.6845	0.0299	-0.0014	-0.0339	56619.4231	26.0449	0.0204	-32.0577	0.0268	-0.0975	0.0049
56619.2736	-74.8908	0.0075	-52.3081	0.0177	0.0033	0.0192	56890.5147	32.8145	0.0242	-40.7347	0.0288	0.0780	-0.0049
56890.4483	-50.3115	0.0067	-79.8551	0.0221	-0.0060	-0.0002	57159.5852	23.8836	0.0215	-29.1134	0.0249	-0.0255	0.0137
57073.6986	-50.2649	0.0077	-79.8382	0.0248	0.0093	0.0518	57160.5816	18.7741	0.0229	-22.2593	0.0302	0.0997	-0.0127
57159.5432	-73.8810	0.0079	-53.3993	0.0257	0.0044	0.0573							
57295.3098	-76.9201	0.0069	-50.1277	0.0290	-0.0122	-0.0548							

**Table 4.** Correction terms applied to the uncertainties of the previous and of the new RV measurements. The composition of these terms into a uncertainty correction is explained in Section 4.1, eqs. 1 and 2.

HIP	Reference of previous RV	Correction terms for previous measurements				Correction terms for new measurements			
		$\varepsilon_{1,p}$	$\varphi_{1,p}$	$\varepsilon_{2,p}$	$\varphi_{2,p}$	$\varepsilon_{1,n}$	$\varphi_{1,n}$	$\varepsilon_{2,n}$	$\varphi_{2,n}$
		km s <sup>-1</sup>		km s <sup>-1</sup>		km s <sup>-1</sup>		km s <sup>-1</sup>	
12081	Griffin (2005)	0	0.615	0	0.565	0.1428	1	0.0061	1
13791	Imbert (2006)	0.24	1	.	.	0.0287	0.885	0.2689	0.885
17732	Griffin & Suchkov (2003)	0	0.272	0	0.759	0	1.101	0.0380	1.101
56275	Griffin (2006)	0	1.208	0	1.208	0.6909	0.905	0.2315	0.905
61727	Halbwachs, Mayor & Udry (2012)	0.3212	1	.	.	0.0261	0.911	0.4914	0.911
62935	Griffin (2004)	0	0.594	.	.	0.0294	1.101	0.1774	1.101
67195	Shajn (1939)	0	5.243	.	.	0.0175	1.046	0	0.8170
87895	McAlister et al. (1995)	0	0.342	0	0.342	0.0355	1.329	0.0662	1.329
95575	Tokovinin (1991)	1.022	1	1	1	0.0108	0.897	0.0399	0.897
100321	Carquillat & Ginestet (2000)	0	0.541	0	1.097	0.0665	1.017	0	0.572

All the RV measurements and the uncertainties used in the derivation of the orbits will be available through the SB9 Catalogue (Pourbaix et al. 2004), which is accessible on-line<sup>1</sup>.

## 4.2 Derivation of the orbital elements

For each binary, we fitted an SB2 orbital model to the previously published datasets combined with the new SOPHIE observations. The parameters were optimized using a Levenberg-Marquard method.

The final orbital solution consists in the following orbital elements: the period,  $P$ , the eccentricity,  $e$ , the epoch of the periastron,  $T_0$ , the longitude of the periastron for the primary component,  $\omega_1$ , the RV semi-amplitudes of each component,  $K_1$  and  $K_2$ , and the RV of the barycentre,  $V_0$ .

We also added 3 supplementary parameters, which are: a systematic offset between the measurements previously published and the new ones,  $d_{n-p}$ , and the offsets between the RVs of the primary and of the secondary component,  $d_{2-1}^p$  and  $d_{2-1}^s$ . The offset  $d_{2-1}^p$  is usually due to

the fact that the published RVs were obtained from templates which are not specifically adapted to each component. For instance, a spectrovelocimeter like CORAVEL (Baranne, Mayor & Poncet 1979) was working by projecting any spectrum on a mask representing the spectrum of Arcurus. The offset between the primary and secondary RVs derived with TODMOR,  $d_{2-1}^m$  is expected to be null, but it is significant for some stars, since the spectra of the PHOENIX library do not perfectly represent the actual ones.

## 4.3 Results

Even with a correction, the uncertainties of the measurements from SOPHIE remain small and have weights much larger than the others. Therefore, incorporating the published datasets in the calculation essentially improved the accuracy of the period determined. Conversely, the significant precision of the new SOPHIE measurements allowed us to reach a very good accuracy on all other orbital parameters, especially the minimum masses.

The derived orbital elements for the 10 SB2 are given in Table 5. Among the 20 component stars, 15 of them have  $M \sin^3 i$  determined with an accuracy better than 0.7 %,

<sup>1</sup> <http://sb9.astro.ulb.ac.be/>

**Table 5.** The orbital elements derived from the previously published RV measurements and from the new ones. The radial velocity of the barycentre,  $V_0$ , is in the reference system of the new measurements of the primary component. The minimum masses and minimum semi-major axes are derived from the true period ( $P_{true} = P \times (1 - V_0/c)$ ).

HIP HD	$P$ (d)	$T_0$ (BJD) 2400000+	$e$	$V_0$ (km s <sup>-1</sup> )	$\omega_1$ (°)	$K_1$ $K_2$ (km s <sup>-1</sup> )	$\mathcal{M}_1 \sin^3 i$ $\mathcal{M}_2 \sin^3 i$ ( $\mathcal{M}_\odot$ )	$a_1 \sin i$ $a_2 \sin i$ (Gm)	$N_1$ $N_2$	$d_{n-p}$ $d_{2-1}^p, d_{2-1}^n$ (km s <sup>-1</sup> )	$\sigma(O_1 - C_1)_{p,n}$ $\sigma(O_2 - C_2)_{p,n}$ (km s <sup>-1</sup> )
12081	443.288	55905.74	0.58494	-7.883	283.66	16.784	0.5493	82.98	47+11	-1.141	0.634,0.128
15850	$\pm 0.023$	$\pm 0.12$	$\pm 0.00054$	$\pm 0.046$	$\pm 0.10$	$\pm 0.057$ 18.258 $\pm 0.015$	$\pm 0.0019$ 0.5050 $\pm 0.0034$	$\pm 0.28$ 90.261 $\pm 0.052$	47+11	$\pm 0.101$ -0.208, -0.064 $\pm 0.124, \pm 0.050$	0.548,0.020
13791	48.70895	55050.392	0.18781	-8.537	55.26	16.030	0.2405	10.5456	33+12	0.686	0.431,0.022
18328	$\pm 0.00023$	$\pm 0.043$	$\pm 0.00078$	$\pm 0.012$	$\pm 0.29$	$\pm 0.015$ 27.07 $\pm 0.14$	$\pm 0.0027$ 0.14241 $\pm 0.00094$	$\pm 0.0090$ 17.809 $\pm 0.089$	0+11	$\pm 0.078$ ..., 0.400 ..., $\pm 0.096$	..., 0.246
17732	277.9500	55230.207	0.14319	-2.918	159.14	18.6644	1.1359	70.598	41+11	-1.096	0.505,0.0080
23626	$\pm 0.0074$	$\pm 0.095$	$\pm 0.00083$	$\pm 0.011$	$\pm 0.14$	$\pm 0.0051$ 23.208 $\pm 0.017$	$\pm 0.0019$ 0.9135 $\pm 0.0010$	$\pm 0.022$ 87.784 $\pm 0.067$	41+11	$\pm 0.058$ 0.279, 0.116 $\pm 0.169, \pm 0.027$	1.670,0.054
56275	47.89410	56781.809	0.2317	-17.879	247.52	28.00	1.5007	17.94	31 <sup>a</sup> +13	-1.273	1.299,0.571
100215	$\pm 0.00089$	$\pm 0.080$	$\pm 0.0018$	$\pm 0.18$	$\pm 0.71$	$\pm 0.18$ 51.709 $\pm 0.087$	$\pm 0.0086$ 0.8126 $\pm 0.0090$	$\pm 0.11$ 33.128 $\pm 0.051$	10+13	$\pm 0.294$ 0.963, 0.273 $\pm 1.247, \pm 0.202$	3.786,0.207
61727	54.87864	56476.6509	0.34744	-1.5628	185.679	30.842	1.432	21.823	43+12	0.168	0.639,0.020
110025	$\pm 0.00018$	$\pm 0.0072$	$\pm 0.00051$	$\pm 0.0093$	$\pm 0.057$	$\pm 0.019$ 48.51 $\pm 0.26$	$\pm 0.017$ 0.9104 $\pm 0.0060$	$\pm 0.011$ 34.33 $\pm 0.18$	0+12	$\pm 0.097$ ..., 0.358 ..., $\pm 0.142$	..., 0.435
62935	139.0081	55680.66	0.1508	0.244	31.37	15.643	0.4791	29.557	89+11	-0.189	0.680,0.022
112138	$\pm 0.0027$	$\pm 0.17$	$\pm 0.0018$	$\pm 0.011$	$\pm 0.44$	$\pm 0.023$ 23.03 $\pm 0.11$	$\pm 0.0049$ 0.3254 $\pm 0.0020$	$\pm 0.038$ 43.51 $\pm 0.20$	0+11	$\pm 0.065$ ..., 0.416 ..., $\pm 0.071$	..., 0.245
67195	39.284974	56211.2841	0.78584	-9.532	325.250	45.44	1.1731	15.181	37+14	-1.113	5.027,0.021
120005	$\pm 0.000091$	$\pm 0.0045$	$\pm 0.00050$	$\pm 0.016$	$\pm 0.031$	$\pm 0.12$ 78.86 $\pm 0.22$	$\pm 0.0062$ 0.6760 $\pm 0.0034$	$\pm 0.026$ 26.346 $\pm 0.048$	0+14	$\pm 0.864$ ..., -0.013 ..., $\pm 0.050$	..., 0.118
87895	881.629	55650.40	0.4165	-32.346	135.47	11.393	0.9869	125.57	106+14	0.456	0.842,0.035
163840	$\pm 0.065$	$\pm 0.49$	$\pm 0.0014$	$\pm 0.015$	$\pm 0.26$	$\pm 0.021$ 17.374 $\pm 0.077$	$\pm 0.0097$ 0.6471 $\pm 0.0041$	$\pm 0.22$ 191.50 $\pm 0.84$	16+13	$\pm 0.047$ -0.754, 0.319 $\pm 0.608, \pm 0.058$	1.210,0.210
95575	166.8351	56087.993	0.13698	-64.2928	63.21	14.0202	0.23291	31.866	23+12	0.394	1.225,0.0098
183255	$\pm 0.0031$	$\pm 0.094$	$\pm 0.00031$	$\pm 0.0040$	$\pm 0.20$	$\pm 0.0048$ 15.696 $\pm 0.016$	$\pm 0.00051$ 0.20804 $\pm 0.00028$	$\pm 0.011$ 35.675 $\pm 0.037$	9+12	$\pm 0.233$ 0.356, 0.097 $\pm 0.592, \pm 0.014$	1.981,0.044
100321	37.939920	56254.291	0.18242	0.941	111.043	34.306	1.06199	17.596	52+11	0.324	0.530,0.068
195850	$\pm 0.000081$	$\pm 0.010$	$\pm 0.00025$	$\pm 0.023$	$\pm 0.096$	$\pm 0.025$ 45.0916 $\pm 0.0089$	$\pm 0.00081$ 0.8080 $\pm 0.0011$	$\pm 0.013$ 23.1284 $\pm 0.0041$	49+11	$\pm 0.079$ 0.493, 0.121 $\pm 0.174, \pm 0.028$	1.160,0.011

<sup>a</sup> The 3 first measurements in Griffin (2006) were discarded.

while only 5 stars have minimum mass accuracies between 1 and 1.2%.

A comparison between the standard deviation of the residuals of the previous measurements and of the new ones also illustrates the improvements due to SOPHIE. It results from the last column of Table 5 that  $\sigma(O - C)_p$  is between 2.3 and 239 times larger than  $\sigma(O - C)_n$ , with a median around 30.

The orbital solutions, including previously published measurements, are displayed on Fig. 1. The  $(O - C)$  residuals are included in Table 3 and are plotted on Fig. 2. We do not observe any drift for any of the 10 SB2.

## 5 COMBINED ORBITAL SOLUTION AND MASSES FOR HIP 87895

HIP 87895 is the close visual binary (VB) MCA 50. Among the many observations recorded in the on-line *Fourth Catalogue of Interferometric Measurements of Binary Stars*<sup>2</sup>, we found 3 very accurate long-base interferometric measurements performed with the *Palomar Testbed Interferometer* (PTI). Since the RV measurements are already providing parameters common to the spectroscopic and to the visual orbits, three 2-dimension measurements are quite sufficient to derive the remaining ones, which are: the orbital inclination,  $i$ , the position angle of the nodal line,  $\Omega$ , and the ap-

<sup>2</sup> <http://ad.usno.navy.mil/wds/int4.html>

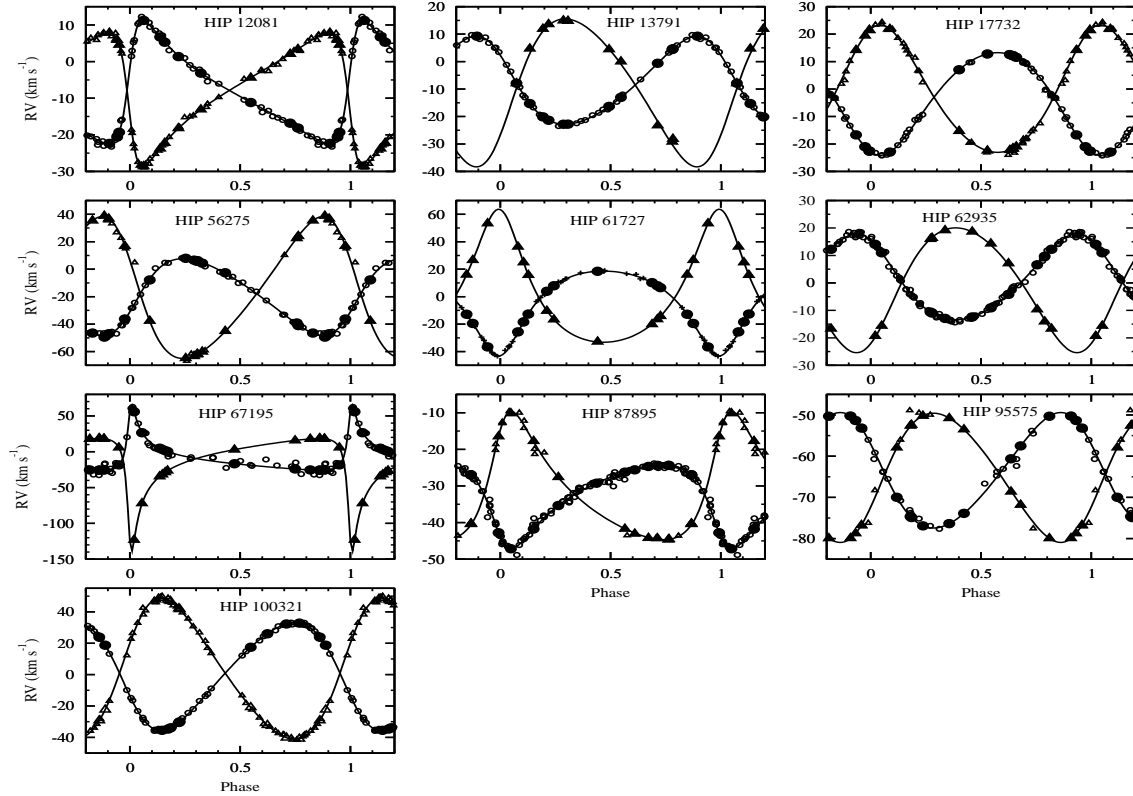


**Figure 1.** The spectroscopic orbits of the 10 SB2; the circles refer to the primary component, and the triangle to the secondary; the large filled symbols refer to the new RV measurements obtained with SOPHIE. For each SB2, the RVs are shifted to the zero point of the SOPHIE measurements of the primary component.

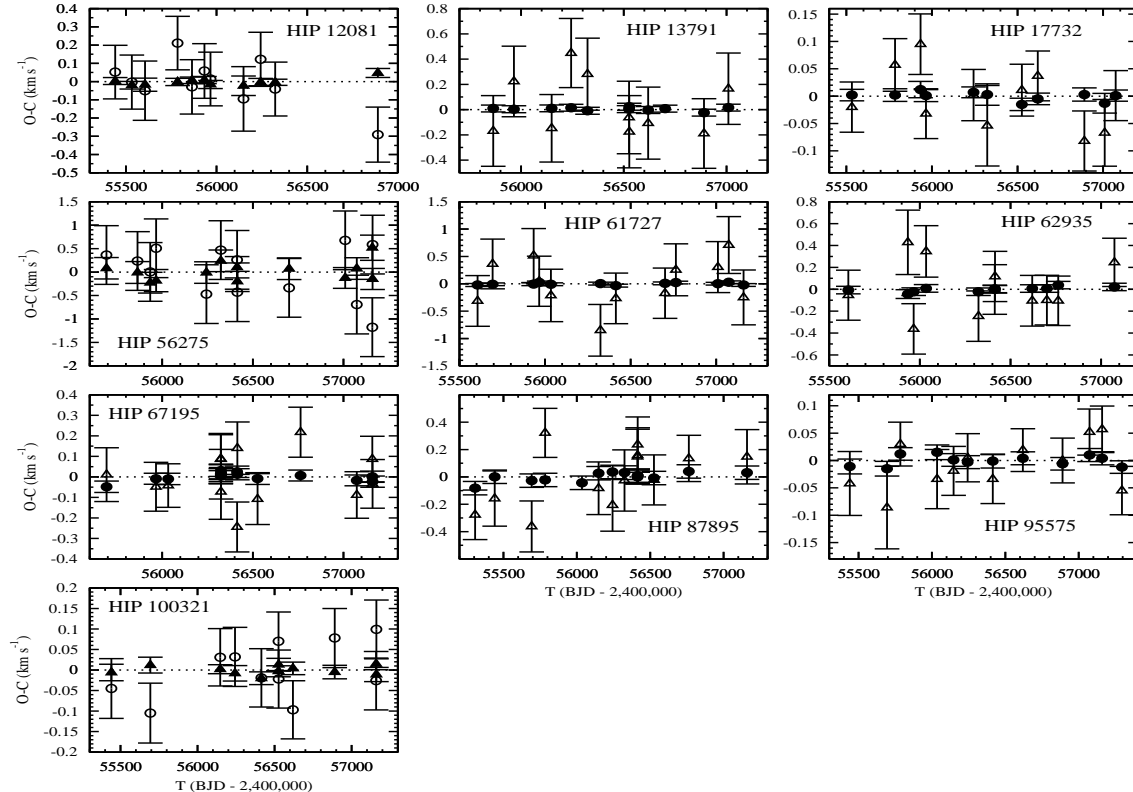


**Figure 2.** The residuals of the RVs obtained from TODMOR for the 10 SB2s. The circles refer to the primary component, and the triangles to the secondary component. For readability, the residuals of the most accurate RV measurements are in filled symbols.

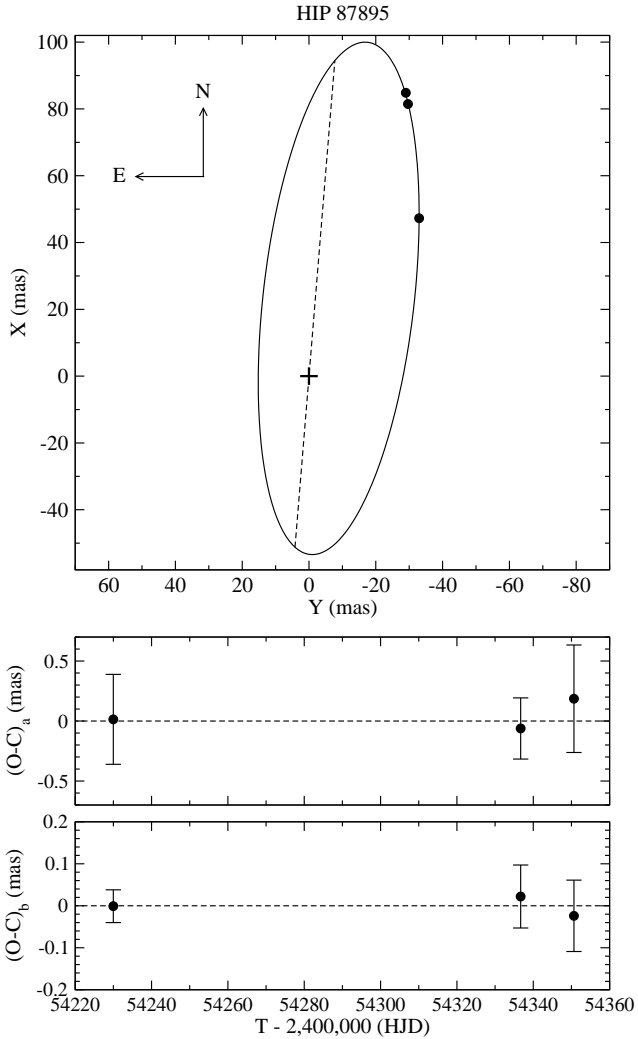


**Figure 3.** The visual part of the combined orbit of HIP 87895. Upper panel: the visual orbit; the circles are the 3 positions obtained from long-base interferometry; the node line is in dashes. Middle panel: the residuals along the semi-major axis of the error ellipsoid. Lower panel: the residuals along the semi-minor axis of the error ellipsoid.

parent semi-major axis or the trigonometric parallax (both may equally be used).

These measurements and the rescaled error ellipsoids provided by Muterspaugh et al. (2010) are taken into account simultaneously with our RV measurements, in order to directly derive the masses of the components and the trigonometric parallax of the system.

The results are given in Table 6, and in Fig. 3. We derived the two masses with accuracies of 1.2 and 0.98 %, respectively.

## 6 SUMMARY AND CONCLUSION

We obtained for 10 SB2 new radial velocity measurements from spectra taken with SOPHIE, among which four new SB2 identified in paper I. The TODMOR algorithm was used to separate the two components in each spectrum. All ten systems had previously published measurements in archive,

**Table 6.** The combined VB+SB2 solutions of HIP 87895; For consistency with the SB orbits and with the forthcoming astrometric orbit,  $\omega$  refer to the motion of the primary component.

HIP 87895	
$P$ (days)	$881.628 \pm 0.064$
$T_0$ (BJD-2400000)	$55650.39 \pm 0.38$
$e$	$0.4165 \pm 0.0010$
$V_0$ ( $\text{km s}^{-1}$ )	$-32.347 \pm 0.014$
$\omega_1$ ( $^\circ$ )	$135.46 \pm 0.16$
$\Omega$ ( $^\circ$ ; eq. 2000)	$175.32 \pm 0.44$
$i$ ( $^\circ$ )	$72.83 \pm 0.47$
ex $a$ (mas)	80.64
$\mathcal{M}_1$ ( $M_\odot$ )	$1.132 \pm 0.014$
$\mathcal{M}_2$ ( $M_\odot$ )	$0.7421 \pm 0.0073$
$\varpi$ (mas)	$36.35 \pm 0.20$
$d_{n-p}$ ( $\text{km s}^{-1}$ )	$0.456 \pm 0.047$
$d_{2-1 p}$ ( $\text{km s}^{-1}$ )	$-0.754 \pm 0.608$
$d_{2-1 n}$ ( $\text{km s}^{-1}$ )	$0.320 \pm 0.056$
$\sigma_{(o-c) V L T I}$ (mas)	0.086
$\sigma_{(o-c) R V p}$ ( $\text{km s}^{-1}$ )	0.841, 1.211
$\sigma_{(o-c) R V n}$ ( $\text{km s}^{-1}$ )	0.035, 0.209

which we added to our measurements to calculate the orbital solutions. We also derived estimations of stellar parameters obtained by optimizing the two dimensional cross-correlation obtained with TODMOR.

We achieved the objective of deriving minimum mass with an accuracy better than 1% for 15 of the 20 stars of our SB2 sample. Moreover, all ten binaries have the minimum mass of both components estimated with relative uncertainties lower than 1.2%. This is a great achievement of the combination of TODMOR and SOPHIE. Especially it did very well in extreme configurations such as with small SNR ( $\sim 40$ ), and very small flux ratio ( $\alpha < 0.05$ ) between the two components.

We combined our RV measurements of HIP 87895 with 3 relative positions derived from long-based interferometric observations, and we obtained new mass estimate of the components,  $M_1 = 1.132 \pm 0.014 M_\odot$  and  $M_2 = 0.7421 \pm 0.0073 M_\odot$ . On the basis of speckle observations, McAlister et al. (1995) previously derived  $M_1 = 1.16 \pm 0.12 M_\odot$  and  $M_2 = 0.77 \pm 0.05 M_\odot$ , i.e. with relative errors of 10 and 6 %. Therefore, our measurements refine profitably to the 1% level the confidence range on the masses of HIP 87895.

Added to the systems observed with PIONIER, we have now 3 binaries observed with SOPHIE which may be used to check the masses that will be derived from GAIA.

## ACKNOWLEDGMENTS

This project was supported by the french INSU-CNRS ‘‘Programme National de Physique Stellaire’’ and ‘‘Action Spécifique Gaia’’. We are grateful to the staff of the Haute-Provence Observatory, and especially to Dr F. Bouchy, Dr H. Le Coroller, Dr M. Véron, and the night assistants, for their kind assistance. We made use of the SIMBAD database, operated at CDS, Strasbourg, France. This research has received funding from the European Community’s Seventh Framework Programme (FP7/2007-2013) under grant-agreement numbers 291352 (ERC). The authors

are very thankful to the anonymous reviewer for his help to improve the quality of this paper.

## REFERENCES

- Baranne A., Mayor M., Poncet J. L., 1979, *VA*, 23, 279  
 Carquillat J.-M., Ginestet N., 2000, *A&AS* 144, 317  
 Griffin R.F., 2004, *The Obs.* 124, 371  
 Griffin R.F., 2005, *The Obs.* 125, 367  
 Griffin R.F., 2006, *The Obs.* 126, 19  
 Griffin R.F., Suchkov A.A., 2003, *ApJSS* 147, 103  
 Halbwachs J.L., Mayor M., Udry S., 2012, *MNRAS* 422, 14  
 Halbwachs J.L., Arenou F., Pourbaix D., Famaey B., Guillout P. et al., 2014, *MNRAS* 445, 2371  
 Halbwachs J.L., Boffin H.M.J., Le Bouquin J.-B., Kiefer F., Famaey B. et al., 2016, *MNRAS* 455, 3303  
 Husser T.-O. et al., 2013, *A&A*, 553, A6  
 Hodgson R.M., Bailey D.G., Naylor M.J., Ng A.L.M., McNeil S.J., 1985, *Image Vision Comput.*, 3(1), 4-14  
 Imbert M., 2006, *Rom. Astron. J.* 16,3  
 Lebreton, Y., 2005, *The Three-Dimensional Universe with Gaia*, 576, 493  
 McAlister H.A., Hartkopf W.I., Mason B.D., Fekel F.C., Ianna P.A., Tokovinin A.A., Griffin R.F., Culver R.B., 1995, *AJ* 110, 366  
 Muterspaugh M.W., Lane B.F., Kulkarni S.R., Konacki M., Burke B.F. et al., 2010, *AJ* 140, 1579  
 Pourbaix D., Tokovinin A. A., Batten A. H., Fekel F. C., Hartkopf W. I., Levato H., Morell N. I., Torres G., Udry S., 2004, *A&A*, 424, 727  
 Shajn G.A., 1939, *Pulkovo Circ.* 25, 26  
 Stuart A., Ord K., 1994, *Kendall's Advanced Theory of Statistics*, vol. 1. Edward Arnold, London  
 Tokovinin, A. A., 1991, *A&AS*, 91, 497  
 Torres G., Fischer D. A., Sozzetti A., Buchhave L. A., Winn J. N., Holman M. J., Carter J. A., 2012, *ApJ*, 757, 161  
 Zucker S., Mazeh T., 1994, *ApJ*, 420, 806  
 Zucker S., Mazeh T., Santos N. C., Udry S., Mayor M., 2004, *A&A*, 426, 695

This paper has been typeset from a  $\text{\LaTeX}$  file prepared by the author.